Eur. Phys. J. B **37**, 439–446 (2004)
DOI: 10.1140/epjb/e2004-00079-y

THE EUROPEAN PHYSICAL JOURNAL B

On the nature of the magnetic transition in a Mott insulator*

M. Fleck[1], A.I. Lichtenstein[2], M.G. Zacher[3], W. Hanke[3], and A.M. Oleś[1,4,a]

[1] Max-Planck-Institut für Festkörperforschung, Heisenbergstrasse 1, 70569 Stuttgart, Germany
[2] University of Nijmegen, Toernooiveld 1, 6525 ED Nijmegen, The Netherlands
[3] Institut für Theoretische Physik und Astrophysik, Universität Würzburg, Am Hubland, 97074 Würzburg, Germany
[4] Marian Smoluchowski Institute of Physics, Jagellonian University, Reymonta 4, 30059 Kraków, Poland

Received 21 August 2003 / Received in final form 20 November 2004
Published online 9 April 2004 –

Abstract. Using a combination of exact enumeration and the dynamical mean-field theory (DMFT) we study the drastic change of the spectral properties, obtained in the half-filled two-dimensional Hubbard model at a transition from an antiferromagnetic to a paramagnetic Mott insulator, and compare it with the results obtained using the quantum Monte Carlo method. The coherent hole (electron) quasiparticle spin-polaron subbands are gradually smeared out when the AF order disappears, either for increasing Coulomb repulsion U at fixed temperature T, or for increasing T at fixed U. Within the DMFT we present numerical evidence (a continuous disappearence of the order parameter) suggesting that the above magnetic transition is second order both in two and in three dimensions.

PACS. 71.30.+h Metal-insulator transitions and other electronic transitions – 71.10.Fd Lattice fermion models (Hubbard model, etc.) – 79.60.-i Photoemission and photoelectron spectra

1 Introduction

The nature of the magnetic transition from a paramagnet to an antiferromagnet in a Mott insulator is one of the fundamental problems in the physics of strongly correlated systems [1]. Such transitions are found in numerous Mott insulators as a function of chemical pressure, as for instance in $V_{2-x}Cr_xO_3$ [2]. Only recently the Mott transition in V_2O_3 could be analyzed within a sophisticated and realistic approach, which includes the orbital degrees of freedom, by combining the local density approximation with a many-body dynamical mean-field theory (DMFT) [3]. In an insulating phase one might attempt to understand the magnetic transition using the Heisenberg model for localized spins. However, close to the Mott transition the electron localization is far from perfect, and an explicit description of the charge degrees of freedom of strongly correlated $3d$ electrons in magnetic states is required.

The generic features of the magnetic transition in a Mott-Hubbard insulator without orbital degrees of freedom, such as for instance La_2CuO_4, are expected to be explainable in terms of the half-filled ($n = 1$) single band Hubbard model [4], which describes electron hopping on a lattice with nearest-neighbor element t (taken as an energy unit $t = 1$) interacting with each other through an on-site Coulomb repulsion U. In a Mott insulator at $U \gg t$, the high-energy scale $\propto U$ determines the insulating (charge) gap at half-filling. The charge fluctuations between two neighboring sites are then realized only as virtual $d_i^1 d_j^1 \rightleftharpoons d_i^2 d_j^0$ transitions which lead to the antiferromagnetic (AF) exchange interaction J of the order of t^2/U (in a strongly correlated regime $J = 4t^2/U$). These transitions determine the low-energy scale $\propto J$ and are the source of strong AF correlations near and at half-filling, being short-range in a two-dimensional (2D) system, but leading to the long-range order (LRO) below the Néel temperature T_N in a three-dimensional (3D) system.

The spectral properties depend on both above energy scales and can be correctly reproduced only when the respective Green's functions are determined with sufficient accuracy. In the high temperature regime when charge fluctuations are still suppressed ($U \gg k_BT \gg J$), the lower and upper Hubbard subbands are reproduced within the quantum Monte Carlo (QMC) method not only at half-filling, but also in weakly doped regime [5–7]. One finds that, up to some minor modifications, the band structure is consistent with the Hubbard I predictions [7], which amounts to the neglect of *intersite spin correlations*, i.e., the system is in a spin disordered state. However, at low temperature ($k_BT \simeq J$) this method gives in addition the quasiparticle (QP) bands on the top of the lower Hubbard band and on the bottom of the upper Hubbard

* This work is dedicated to Professor Ole Krogh Andersen on the occasion of his 60th birthday.

[a] e-mail: a.m.oles@fkf.mpg.de

band, respectively [5]. These bands can be reproduced in analytic methods only when spin correlations are explicitly included [7,8].

An alternative approach is the DMFT [9], which provides the exact solution of the Hubbard model in the limit of infinite dimension [10]. The DMFT has been very successful in describing various aspects of strongly correlated systems [9], including local correlations in magnetically ordered phases [11]. At $n = 1$ it reproduces rather accurately the charge gap $\propto U$, and gives the spectral function in excellent agreement with the exact diagonalization of finite clusters [12]. The low-energy scale $\propto J$ is there obtained as well, and this result appears to be consistent with the retracable path approximation of Brinkman and Rice [13], which becomes exact in the limit of $d \to \infty$ [14].

It was established by recent studies that the metal-insulator transition within the paramagnetic (PM) phase is first order at finite temperature [15]. A discontinuous transition with hysteresis was found within the DMFT, using either exact diagonalization [16,17], or numerical renormalization group [18]. However, a continuous metal-insulator transition was found at $T = 0$ in a cluster approach [19], and within the random dispersion approximation [20]. In fact, two solutions to the DMFT equations exist at $T = 0$ in the PM phase (often loosely referred to as hysteresis), but this does not imply yet that the transition is first order. As we will show below, the situation is somewhat similar for the magnetic transition within an insulating phase, where two solutions of the DMFT equations exist at finite temperature.

The magnetic transition *within the insulating phase* was even less investigated. It is driven by the low-energy spin excitations $\propto J$, and occurs at temperatures well below the metal-insulator transition in a 3D model [21–24]. Also in a 2D model the characteristic temperature below which the spin correlations are stable $T^* \propto T_N^{\rm MF} = J$, where $T_N^{\rm MF}$ is the Néel temperature obtained in the mean-field approximation for the Heisenberg antiferromagnet, is lower than the one that corresponds to the suppression of charge fluctuations at the metal-insulator transition, in strong coupling [25], and even in the weak coupling regime [26].

In this paper, we address the problem of the evolution of the spectral properties in the half-filled Hubbard model at a transition from an AF to a PM Mott insulator. We show below that the excitation spectra are drastically modified at the magnetic transition. The quality of the self-energy is of crucial importance for investigating the magnetic states [11], as its inaccurate form might easily destabilize the magnetic order. Therefore, we have adopted the DMFT combined with exact enumeration [9] to investigate the magnetic states. In the present study we used up to 26 time slices which is numerically quite extensive, but gives sufficient accuracy. We compare the results of this approach applied to a 2D Hubbard model with those obtained using directly the QMC method itself [27], called below 2D-QMC. This method provides an independent check on the accuracy of the DMFT approach, and on the quality of the obtained self-energy. We investigate the nature of the transition at finite temperature from the regime with pronounced AF correlations to a paramagnet by evaluating the double occupancy and the staggered order parameter using the DMFT method. Altogether, our results show that the DMFT is very sensitive to the local correlations, and predicts the second order magnetic phase transition within the insulating phase.

The paper is organized as follows. In Section 2 we summarize the formalism and the method to determine the spectral function within the DMFT. The numerical results obtained within the DMFT are presented and discussed in Section 3. They are also compared with the 2D-QMC calculation, and we present evidence that the magnetic transition in the Hubbard model is second order. The discussion of the obtained hysteresis in the double occupancy, the magnetic transition and the Néel temperature in the 3D Hubbard model, and the main conclusions are presented in Section 4.

2 Spectral function within the DMFT

We consider the 2D Hubbard model at half-filling with hopping t between the nearest neighbors $\langle ij \rangle$,

$$H = -t \sum_{\langle ij \rangle, \sigma} c_{i\sigma}^{\dagger} c_{j\sigma} + U \sum_i \left(n_{i\uparrow} - \frac{1}{2} \right) \left(n_{i\downarrow} - \frac{1}{2} \right). \quad (1)$$

While the local spin quantization axis determined by spin order is site dependent in spiral phases in doped systems ($n \neq 1$) [28], it is fixed in the AF phase, stable at $n = 1$ in the low temperature regime. We write the staggered magnetization in the AF phase, $\langle S_i^z \rangle = \frac{1}{2} \langle n_{i\uparrow} - n_{i\downarrow} \rangle = m \exp(i \mathbf{R}_i \cdot \mathbf{Q})$, where $\mathbf{Q} = (\pi, \pi)$ characterizes the AF order, which allows to transform the kinetic energy in Hamiltonian (1) to local quantization axes [12],

$$\hat{T}_{\mathbf{Q}}(\mathbf{k}) = \frac{1}{2} \left[\varepsilon_{\mathbf{k}+\mathbf{Q}/2} (\hat{1} + \hat{\sigma}_x) + \varepsilon_{\mathbf{k}-\mathbf{Q}/2} (\hat{1} - \hat{\sigma}_x) \right], \quad (2)$$

where $\varepsilon_{\mathbf{k}} = -2t(\cos k_x + \cos k_y)$ is the band dispersion, and $\hat{\sigma}_x$ is the Pauli matrix.

The lattice Green's function is described by a (2×2) matrix $\hat{G}_{\mathbf{Q}}(\mathbf{k}, i\omega_\nu)$ in spin space, where ω_ν are fermionic Matsubara frequencies. In the spirit of the DMFT approach [9], we approximate the Green's function using a *local self-energy* [10],

$$\hat{G}_{\mathbf{Q}}^{-1}(\mathbf{k}, i\omega_\nu) = i\omega_\nu - \hat{T}_{\mathbf{Q}}(\mathbf{k}) - \hat{\Sigma}_{\mathbf{Q}}(i\omega_\nu). \quad (3)$$

The corresponding local lattice Green's function is $\hat{G}_{\mathbf{Q}}(i\omega_\nu) = \frac{1}{N} \sum_{\mathbf{k}} \hat{G}_{\mathbf{Q}}(\mathbf{k}, i\omega_\nu)$. The solution of the Hubbard model within the DMFT is then determined by the following single-site effective action [29],

$$S_{\mathit{eff}} = -\sum_\sigma \int_0^\beta d\tau d\tau' c_{o\sigma}^{\dagger}(\tau) \mathcal{G}_{\mathbf{Q},\sigma\sigma}^0 (\tau - \tau')^{-1} c_{o\sigma}(\tau') + U \int_0^\beta d\tau \left(n_{o\uparrow}(\tau) - \frac{1}{2} \right) \left(n_{o\downarrow}(\tau) - \frac{1}{2} \right), \quad (4)$$

and by the self-consistency relation:

$$\hat{\mathcal{G}}^0_{\mathbf{Q}}(i\omega_\nu)^{-1} = \hat{G}^{-1}_{\mathbf{Q}}(i\omega_\nu) + \hat{\Sigma}_{\mathbf{Q}}(i\omega_\nu). \quad (5)$$

For the calculation of the single-site Green's function we use exact enumeration [9], and we use ancillary spins (as in the QMC), and the sum over configuations is done exactly in order to solve the DMFT equations self-consistently. Finally, we determine the spectral function using the lattice Green's function for the optimal $\mathbf{Q} = (\pi, \pi)$,

$$A(\mathbf{k}, \omega) = -\frac{1}{\pi} \sum_{\sigma\sigma'} \mathrm{Im}\, G_{\mathbf{Q},\sigma\sigma'}\Big(\mathbf{k} - \frac{1}{2}\mathbf{Q}, \omega + i\epsilon\Big). \quad (6)$$

The resulting $\mathbf{k}$-dependent spectral density is finally plotted using a 64×64 lattice. For comparison, the Green's functions and the spectral functions were determined independently in the direct QMC calculations at finite temperature, and employing the standard maximum entropy technique [5,7].

We begin by investigating the dependence of the lattice Green's function on imaginary time τ for $U = 8t$. By its relation to the spectral function ($\beta = 1/k_B T$) [30],

$$G_{\mathbf{Q}}(\mathbf{k}, \tau > 0) = -\int_{-\infty}^{\infty} d\omega\, \frac{A(\mathbf{k}, \omega) \exp(-\tau\omega)}{1 + \exp(-\beta\omega)}, \quad (7)$$

it allows to conclude whether or not a gap opens at the Fermi energy μ. The behavior of $G_{\mathbf{Q}}(\mathbf{k}, \tau > 0)$ at $\tau \simeq \beta/2$ is crucial, and can be related to the spectral properties by employing equation (7). Indeed, one finds that $G_{\mathbf{Q}}(\mathbf{k}, \beta/2) \simeq 0$ implies that $A(\mathbf{k}, \omega = 0) \simeq 0$. The system is insulating at $U = 8t$ and an AF insulator is stable at low temperature T, but at sufficiently high T the gap around the Fermi level vanishes, and the system crosses over to a strongly correlated metallic regime [7]. This value of U is in the realistic range for high temperature superconductors, and allows us to identify easily both types of the above behavior. Indeed, at $\beta t = 5$ one finds that $G_{\mathbf{Q}}(\mathbf{k}, \tau) \simeq 0$ for $0.25 < \tau/\beta t < 0.75$ even at $X = (\pi, 0)$ and $S = (\pi/2, \pi/2)$ points, which correspond to the edge of the Brillouin zone (BZ) (Fig. 1).

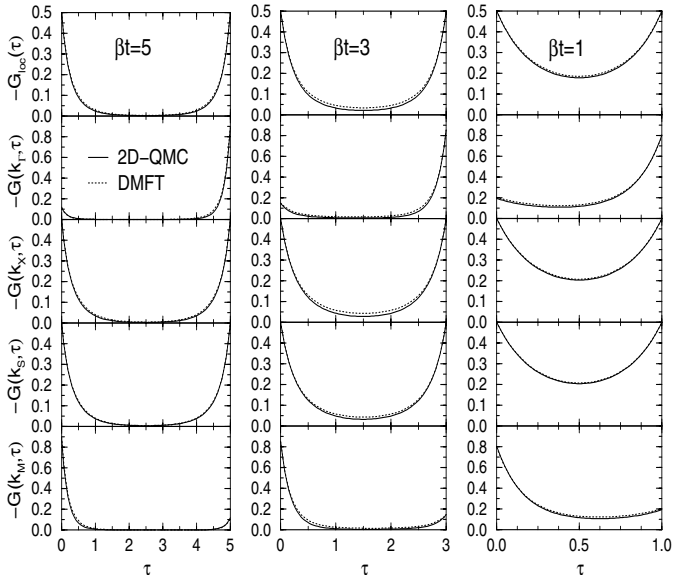

Fig. 1. Green functions: local $-G_{\mathrm{loc}}(\tau)$, and $\mathbf{k}$-dependent $-G(\mathbf{k}, \tau)$, as functions of imaginary time τ (in units of t), at high-symmetry $\mathbf{k}$-points [$\Gamma = (0,0)$; $X = (\pi, 0)$, $S = (\pi/2, \pi/2)$, $M = (\pi, \pi)$], as obtained at $U = 8t$ within the DMFT (dashed lines) and in the 2D-QMC (solid lines), for: the AF insulator with polaron band ($\beta t = 5$, left), the AF insulator within the critical regime ($\beta t = 3$, middle), and the metallic phase of strongly correlated electrons at high temperature above the magnetic transition ($\beta t = 1$, right).

3 Numerical results

3.1 Spectral properties of a Mott insulator

The crossover from an antiferromagnet to a paramagnet with increasing temperature can be identified by analyzing the behavior of the Green's function. As an example we consider intermediate coupling $U = 8t$ which gives $J \simeq 4t^2/U = t/2$. By including the quantum corrections beyond the mean-field theory for the present parameters, Hanke and his collaborators estimated the temperature at which the long-range AF correlations disappear in a quantum 2D system, and found that it satisfies the condition $k_B T^* \leq t/3$ [5,7]. Thus, the long range AF correlations are expected to be lost at $\beta t \simeq 3$. Indeed, increasing T (decreasing β) to $\beta t = 3$ results in finite $G(\mathbf{k}_X, \beta/2)$, but the Green's function $G_{\mathbf{Q}}(\mathbf{k}, \beta/2)$ still vanishes within the majority of the BZ, and thus the gap at the Fermi level persists. However, the spectral function $A(\mathbf{k}, \omega)$ at the X and S points is strongly modified, and the coherent polaronic band is already lost. As we will show in more detail below, this region of temperature corresponds still to a PM insulator. In contrast, when the temperature increases further, a correlated metallic state is found, with finite $G_{\mathbf{Q}}(\mathbf{k}, \beta/2)$ within the entire BZ. The results of the DMFT and the 2D-QMC nearly coincide (see Fig. 1), which demonstrates that the DMFT approach treats the *local correlations* in a very accurate way in the entire parameter regime [31].

Next we analyze the spectral properties in different temperature regimes. The spectral functions found at low T within the DMFT consist of four spectral features: (i) two narrow QP (polaron) bands close to the Fermi energy, at $\omega \simeq \mu$, and (ii) two broader (incoherent) structures which represent two Hubbard subbands. This structure of $A(\mathbf{k}, \omega)$ is generic and agrees very well with that found within the 2D-QMC, as shown in Figure 2. The presence of the polaron QP subbands shows that the local hole-spin dynamics is correctly captured within the DMFT. The QP subbands vanish when the temperature increases, and only two Hubbard subbands separated by the broad gap $\sim U$ can be recognized in the high temperature regime (Fig. 3). Also in this case the DMFT gives a very accurate description of the spectral function. We emphasize that although the system is metallic at $\beta t < 1$

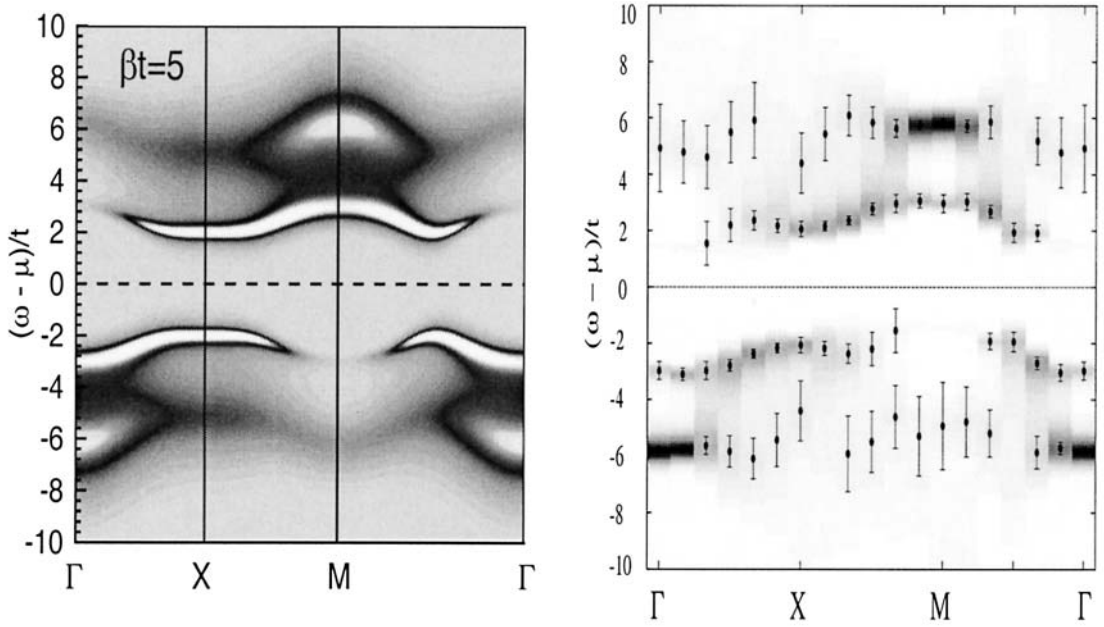

Fig. 2. Spectral function $A(\mathbf{k},\omega)$ of the half-filled Hubbard model at low temperature $\beta t = 5$, with strong antiferromagnetic correlations for $U = 8t$. Left (right) part shows the DMFT (2D-QMC) result. Low spectral weight in the DMFT part is indicated by shadows, while higher weight is shown by white features withing black shadows. The subbands obtained in the 2D-QMD calculations are shown by points with statistical errors, and the shadows stand for their intensities. The high-symmetry points as in Figure 1.

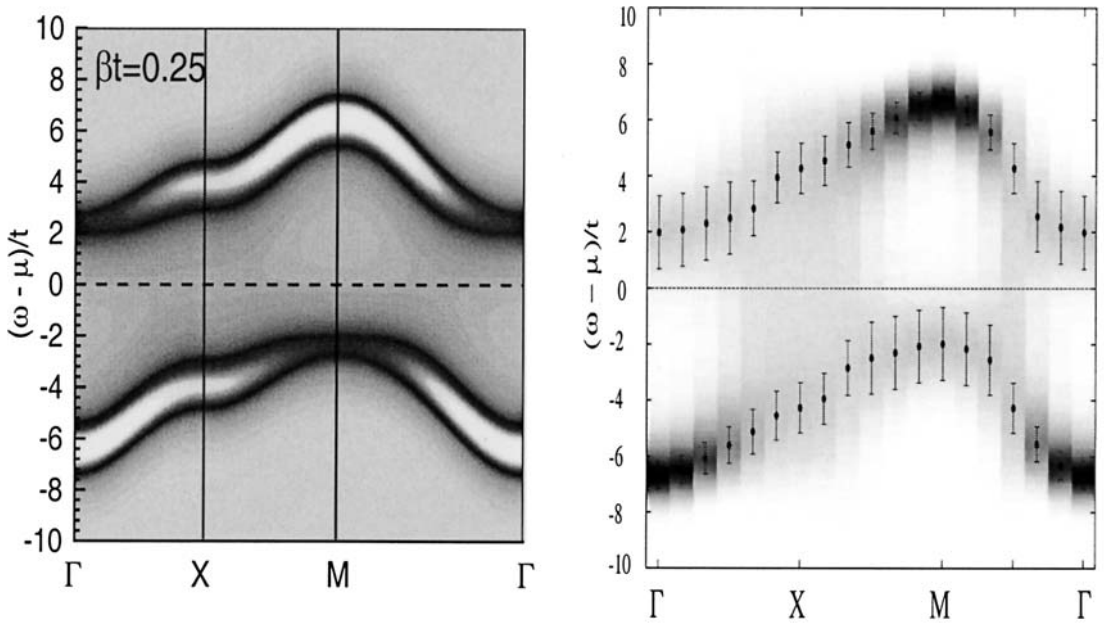

Fig. 3. Spectral function $A(\mathbf{k},\omega)$ as in Figure 2, but for the paramagnetic phase at $\beta t = 0.25$.

for $U = 8t$, and the spectral weight at $\omega = 0$ is finite (in particular close to the X and S points), the spectral function consists of two Hubbard subbands, showing that the charge gap survives in the high temperature regime. In this regime of temperature the local moments are disordered, and their intersite correlations are gradually lost with increasing temperature [23]. Altogether, we have found an excellent agreement between the present analytic DMFT approach and the 2D-QMC method for the distribution of spectral weight and the energy separation between the Hubbard subbands.

The change in the spectral properties found at $U = 8t$ for temperature increasing from $T = t/5$ to $T = t/3$ (in units of $k_B = 1$) is quite drastic. The distinct QP's, well visible close to the Mott-Hubbard gap at $T = t/5$, are lost entirely and replaced by broader structures at

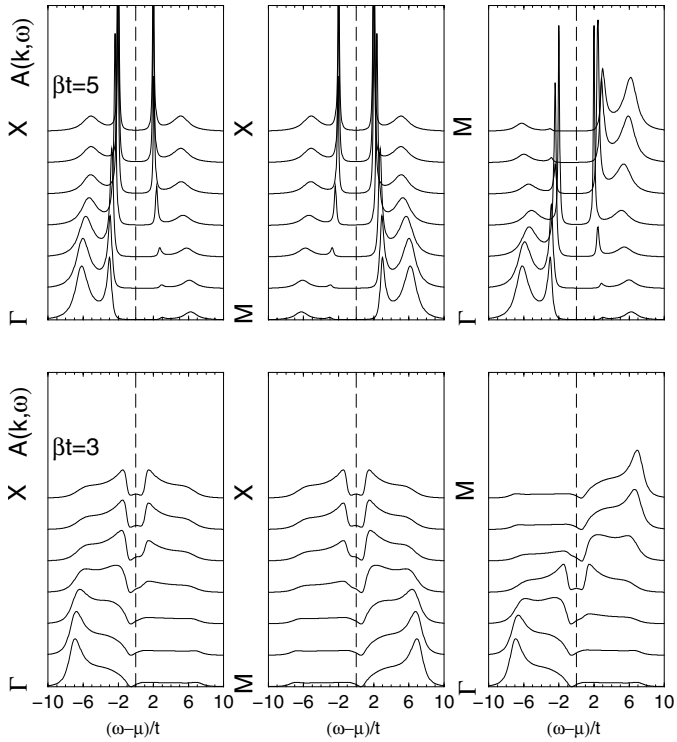

Fig. 4. Spectral function $A(\mathbf{k},\omega)$ as obtained in the DMFT approach along the high-symmetry directions for $U = 8t$ at $\beta t = 5$ (top), and $\beta t = 3$ (bottom). The QP bands are lost at higher temperature $\beta t = 3$. The high-symmetry points as in Figure 1.

$T = t/3$ (Fig. 4). This illustrates that the spin correlations which are weakened with increasing temperature indeed determine the spectral properties. In particular, the coherent QP bands are lost when the long-range AF correlations disappear and the spin correlations become short range, with the correlation length shorter than the cluster size. This interpretation is confirmed by the finite spectral weight found for $\omega \simeq 2t$ at $\beta t = 3$, which originates from the coupling of the hole (electron) to local spin fluctuations. While a hole (an electron) couples coherently to spin fluctuations inducing well formed QP's at the lower temperature $T = t/5$, these processes are to a large extent incoherent at $T = t/3$, which leads to broad spectral structures, reducing even the Mott-Hubbard gap. The decreasing spin order is also indicated by the increased spectral weight at $\omega > 0$ ($\omega < 0$) at and in the vicinity of the Γ (M) point. We emphasize that the low-energy spectral feature still persists but changes to an incoherent peak above the magnetic transition, and vanishes only when the local moments become completely independent of each other at much higher temperature (Fig. 3).

3.2 Magnetic phase transition

Our approach allows to investigate the nature of the magnetic phase transition. It is obtained when increasing U enhances the Mott-Hubbard gap, and suppresses gradually the charge fluctuations. This is best observed by looking at the values of double occupancy $\langle n_{i\uparrow} n_{i\downarrow}\rangle$, shown in Figure 5 for the 2D and 3D Hubbard model in the strongly correlated regime of $U > W$ [where $W = 2zt$ is the bandwidth of the uncorrelated band, and z is the number of nearest neighbors in a square (2D) or cubic (3D) lattice]. The double occupancy is already quite low at $U \simeq W$, with $\langle n_{i\uparrow} n_{i\downarrow}\rangle < 0.05$ ($\langle n_{i\uparrow} n_{i\downarrow}\rangle < 0.03$) for the 2D (3D) model, and gradually decreases with increasing U. Already at $U \simeq W$, the *local moments* for $n = 1$, $\langle \mathbf{S}_i^2\rangle = \frac{3}{4}(1 - 2\langle n_{i\uparrow} n_{i\downarrow}\rangle)$ [32], are well formed and approach fast the limit of electron localization ($\langle \mathbf{S}_i^2\rangle = \frac{3}{4}$). The double occupancy is suppressed somewhat stronger for $U \simeq W$ in the 3D case due to a more pronounced AF order. Therefore, the decrease of $\langle n_{i\uparrow} n_{i\downarrow}\rangle$ with increasing U is here not as fast as in the 2D Hubbard model.

The results obtained for $\langle n_{i\uparrow} n_{i\downarrow}\rangle$ within the 2D-QMC simulations first follow the DMFT values, but at higher values of U are systematically larger. This indicates that in the strongly correlated regime the double occupancy is somewhat underestimated due to a smaller phase space of thermal fluctuations included in the present DMFT method. Although the same temperature is used both in the 2D-QMC and the DMFT, the phase space for charge fluctuations is different. In the DMFT not all but only these paths contribute that scale to one in the limit of $d \to \infty$, and those that have weights $\propto 1/d^{\alpha}$, with $\alpha > 0$ and d standing for the actual dimension, are neglected. Also the magnetic moments are higher in the 2D-QMC, and this enhances the difference in double occupancy between the two methods.

When U increases in the strongly correlated regime of $U > W$, the superexchange interaction $J \simeq 4t^2/U$ decreases, and the intersite magnetic correlations become weaker. When the temperature is fixed, this causes a crossover from the AF to PM phase, with well formed local moments and short-range AF correlations. The results obtained within the DMFT approach allowed us to conclude that this magnetic transition is *second order*, as both the double occupancy $\langle n_{i\uparrow} n_{i\downarrow}\rangle$, and the staggerred magnetization $|\langle S_i^z\rangle| = \frac{1}{2}|\langle n_{i\uparrow} - n_{i\downarrow}\rangle|$, exhibit continuous variation with increasing U. However, when U *decreases*, the PM state is metastable in a range of U, which leads to a jump at $U_c = 11.5t$ ($U_c \simeq 15.4t$) in a 2D (3D) Hubbard model at $\beta t = 3$ in both above quantitities to those obtained in the AF phase. As a result, one finds a distinct *hysteresis* as a function of increasing/decreasing U (Fig. 5) [33]. When U decreases, the ratio of U_c/W at the magnetic transition is somewhat lower in the 3D case ($U_c/W \simeq 1.25t$) than in the 2D model ($U_c/W \simeq 1.44t$), but in both cases electrons are similarly strongly correlated in the regime of $U > U_c$ ($\langle n_{i\uparrow} n_{i\downarrow}\rangle < 0.015$), and the transition (crossover) between the AF and PM phase takes place within the Mott insulator. We emphasize that the magnetic order parameter $|\langle S_i^z\rangle|$ is larger in a 3D than in a 2D system at $U \simeq 1.2W$, and its value is also larger close to U_c when U decreases, demonstrating that the magnetic LRO is robust in a 3D system, in contrast to a 2D system where it appears only due to the symmetry breaking at shorter length scale. This observation follows from the decreasing weight of these

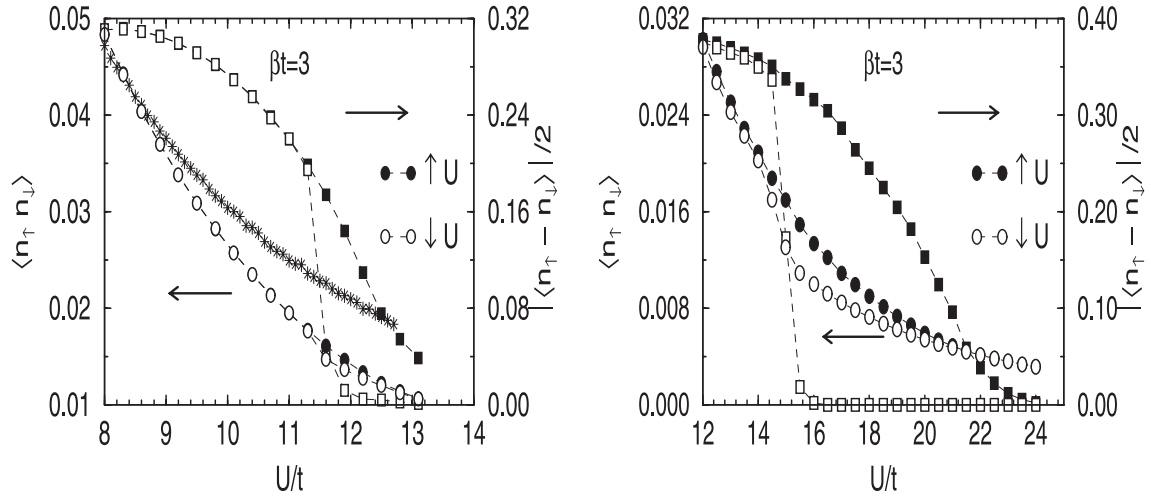

Fig. 5. Double occupancy $\langle n_{i\uparrow}n_{i\downarrow}\rangle$ (circles) and local magnetic moment $|\langle S_i^z\rangle| = \frac{1}{2}|\langle n_\uparrow - n_\downarrow\rangle|$ (squares) as functions of U/t at $\beta t = 3$ obtained in the DMFT for a 2D (left) and 3D (right) Hubbard model, for increasing (filled symbols) and decreasing (empty symbols) U/t. Stars in the left panel show $\langle n_{i\uparrow}n_{i\downarrow}\rangle$ obtained by the 2D-QMC method.

paths which destroy the AF order when the system dimension increases and the classical limit is approached.

The hysteresis in the AF order parameter induces also the hysteresis in the double occupancy. As expected, this latter hysteresis is much smaller as the local moments are already well formed also in the PM states in this range of U, and are only weakly increased when the spin polarization occurs. This behavior is very characteristic of correlated systems [32]; it shows that the local electronic correlations are correctly included within the DMFT approach also in the PM states.

Our conjecture that a second order transition takes place between the AF and PM insulator is further supported by the changes of magnetization found with increasing/decreasing temperature at fixed U. Here we discuss the DMFT data obtained in the 3D case, where the AF LRO is more robust. When temperature decreases, the local moments $|\langle S_i^z\rangle|$ tend to order antiferromagnetically. They show again a distinct hysteresis, now as a function of decreasing (increasing) T; for $U = 16t$ it develops (vanishes) around $T_N^* \simeq 0.35t$ ($T_N \simeq 0.44t$), as shown in Figure 6. When temperature increases, the magnetic moments decrease continuously to zero, and such a behavior is similar to that of a Heisenberg antiferromagnet. We interpret a magnetic transition found at T_N^* when the temperature is lowered as a sudden collapse of the PM state, which is metastable in a range of temperature below T_N: $T_N^* < T < T_N$.

The values of $\langle n_{i\uparrow}n_{i\downarrow}\rangle$ are enhanced by thermodynamic fluctuations at high temperature, and gradually diminish in the PM state when the temperature is reduced (Fig. 6). However, this trend is reversed below T_N^* when the magnetic moments order and double occupancy rapidly increases. This is a clear signature of somewhat enhanced charge fluctuations in the ordered phase. On the contrary, increasing temperature within the magnetically ordered state reduces gradually the phase space for charge fluctuations when the magnetic order parameter $|\langle S_i^z\rangle|$ and the

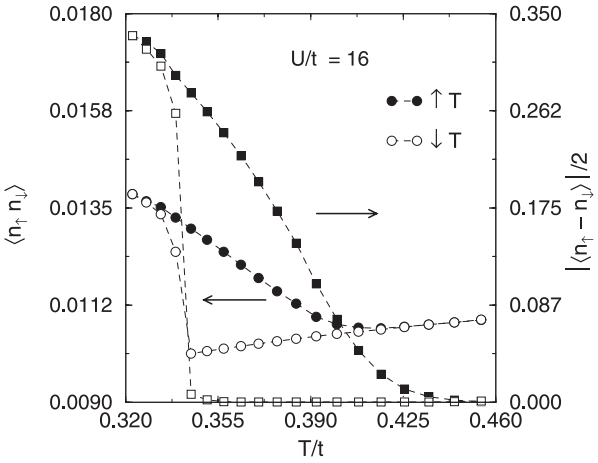

Fig. 6. Double occupancy $\langle n_{i\uparrow}n_{i\downarrow}\rangle$ (circles) and local magnetic moment $|\langle S_i^z\rangle| = \frac{1}{2}|\langle n_\uparrow - n_\downarrow\rangle|$ (squares) as functions of T/t, obtained for the 3D Hubbard model in the DMFT method. Filled and empty symbols correspond to increasing and decreasing T/t, respectively.

double occupancy $\langle n_{i\uparrow}n_{i\downarrow}\rangle$ decrease. In this case the double occupancy passes by its minimum precisely at the magnetic transition (at $T \simeq T_N$), and starts to increase again as the thermal fluctuations gradually increase with T in the PM phase.

4 Discussion and conclusions

It is interesting to ask whether our study concerns indeed the insulating phase. The metal-insulator transition which would take place in the PM phase is hidden by the AF order both in the 2D and in 3D Hubbard model, hence it could not be determined. However, the compressibility which decreases smoothly with U in the 3D Hubbard model [24] indicates that the metal-insulator transition

would take place at $U \simeq 9t$, and a lower value can be expected in the 2D case. Therefore, our analysis of the spectral properties and the magnetic transition was limited to the strongly correlated regime of a Mott insulator.

The present study shows that the magnetic transition is driven by the spin degrees of freedom which modify local correlations when the magnetic order changes. The existence of hysteresis in a range of T and U allows for a direct comparison of the double occupancy in the (stable) AF state with that found in the (metastable) PM state for the same parameters, being a measure of local correlations in both states. Our results demonstrate that the doubly occupied configurations are generated only by virtual charge fluctuations in the strongly correlated regime of $U > W$. While such fluctuations are more frequent in the AF states, they are partly blocked in disordered states, leading therefore to lower values of $\langle n_{i\uparrow} n_{i\downarrow} \rangle$ in the PM states.

Finally, we consider the value of the Néel temperature by itself. Using the superexchange interaction $J = 4t^2/U$ (as obtained in the limit of large U), and neglecting the intersite spin correlations, as done within the Weiss molecular field theory for the Heisenberg model, one finds $T_N^{\rm MF} = 6t^2/U$. While the early QMC data [21,22] come close to $T_N^{\rm MF}$, more recent QMC calculations included as well *intersite quantum fluctuations* and gave thus lower values of T_N [24] (Fig. 7). In this latter case the QMC results are close to the empirical value of T_N expected for a 3D quantum antiferromagnet [34],

$$k_B T_N^{\rm emp} = \frac{5}{192}[11S(S+1) - 1](z-1)J, \qquad (8)$$

where z is the number of nearest neighbours (here $z = 6$), and S is spin quantum number. We note that indeed $T_N^{\rm emp}$ reproduces within less than 0.3% the value of $T_N = 0.946J$ found from the finite size scaling of the QMC data obtained for the 3D $S = \frac{1}{2}$ Heisenberg antiferromagnet [35], and both results are indistinguishable from each other in Figure 7.

By its nature, the present DMFT calculations do not include the intersite quantum fluctuations, and thus give the magnetic transition at temperature close to $T_N^{\rm MF}$. The latter value falls close to the center of the hysteresis curve found both at $T = t/3$ and at $U = 16t$ (Fig. 7), and shows that the charge fluctuations play still some role in the strong coupling regime characterized by $T_N \propto t^2/U$, enhancing the value of T_N. However, the charge fluctuations would be entirely suppressed in the limit $U \to \infty$, and the DMFT would then reduce precisely to the Weiss molecular field theory of the Heisenberg model. Therefore, the volume inside the hysteresis tends to zero with increasing $U \to \infty$, when two temperatures identified in our calculation (T_N and T_N^*) decrease and would finally merge and give just $T_N^{\rm MF}$ as obtained for the Heisenberg model. This supports our interpretation of the hysteresis, being a signature of the *itinerant behavior* consistent with the second order magnetic phase transition.

Summarizing, we have demonstrated that the spectral properties of the half-filled Hubbard model change in a drastic way at the magnetic transition from an *antiferromagnetic* to a *paramagnetic* Mott insulator. While in the high temperature regime ($J < k_B T \ll U$) the system is characterized by two Hubbard subbands separated by a gap $\propto U$, these bands loose partly their spectral weights, and the polaron QP subbands emerge simultaneously at low energy $\propto J$ in the low temperature regime ($k_B T < J$). Using the DMFT method combined with exact enumeration we could establish that the order-disorder magnetic phase transition in a Mott insulator is second order, and is driven by the spin degrees of freedom.

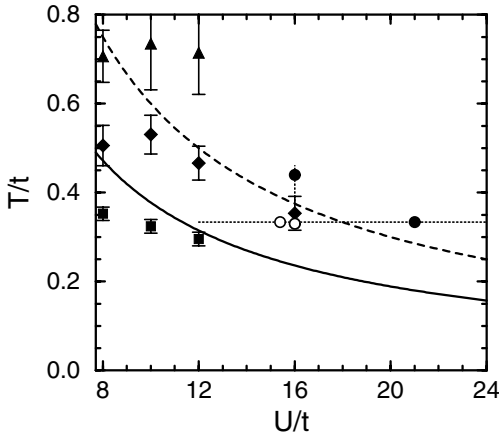

Fig. 7. Magnetic phase diagram of the half-filled 3D Hubbard model in the strong coupling regime $U \geq 8t$. Data points (with error bars) show the Néel temperature T_N as function of U/t obtained in various QMC calculations: filled triangles [21], filled diamonds [22], filled squares [24]. The present DMFT calculations with results shown in Figures 5 and 6 were performed along dotted lines, and the magnetic phase transition was found at T_N (T_N^*) either for increasing (decreasing) U/t or for increasing (decreasing) T, as shown by filled (empty) circles. The value of $T_N^{\rm MF}$ obtained from the Weiss molecular field theory for $S = \frac{1}{2}$ Heisenberg antiferromagnet with $J = 4t^2/U$, and the expected experimental value $k_B T_N^{\rm emp}$ equation (8), are shown by dashed and solid line, respectively.

We thank K. Held and D. Vollhardt for valuable discussions and for their insightful comments. One of us (W.H.) would like to thank O.K. Andersen and the Max-Planck-Institut für Festkörperforschung for support and generous hospitality during his stay at the Institute which stimulated this work. A.M.O. acknowledges the support by the Polish State Committee of Scientific Research (KBN), Project No. 5 P03B 055 20.

References

1. M. Imada, A. Fujimori, Y. Tokura, Rev. Mod. Phys. **70**, 1039 (1998)
2. D.B. McWhan, A. Menth, J.P. Remeika, W.F. Brinkman, T.M. Rice, Phys. Rev. Lett. **27**, 941 (1971); W. Bao, C. Broholm, G. Aeppli, P. Dai, J.M. Honig, P. Metcalf, Phys. Rev. Lett. **78**, 507 (1997); W. Bao, C. Broholm, G. Aeppli, S.A. Carter, P. Dai, T.F. Rosenbaum, J.M. Honig, P. Metcalf, S.F. Trevino, Phys. Rev. B **58**, 12727 (1998)

3. K. Held, G. Keller, V. Eyert, D. Vollhardt, V.I. Anisimov, Phys. Rev. Lett. **86**, 5345 (2002)
4. J. Hubbard, Proc. Roy. Soc. Lond. A **276**, 238 (1963)
5. R. Preuss, W. Hanke, W. von der Linden, Phys. Rev. Lett. **75**, 1344 (1995)
6. M. Ulmke, M.T. Scalettar, A. Nazarenko, E. Dagotto, Phys. Rev. B **54**, 16523 (1996)
7. C. Gröber, R. Eder, W. Hanke, Phys. Rev. B **62**, 4336 (2000)
8. A. Dorneich, M.G. Zacher, C. Gröber, R. Eder, Phys. Rev. B **61**, 12816 (2000)
9. A. Georges, G. Kotliar, W. Krauth, M.J. Rozenberg, Rev. Mod. Phys. **68**, 13 (1996)
10. W. Metzner, D. Vollhardt, Phys. Rev. Lett. **62**, 324 (1989)
11. M. Fleck, A.I. Lichtenstein, E. Pavarini, A.M. Oleś, Phys. Rev. Lett. **84**, 4962 (2000)
12. M. Fleck, A.I. Lichtenstein, A.M. Oleś, L. Hedin, V.I. Anisimov, Phys. Rev. Lett. **80**, 2393 (1998)
13. W.F. Brinkman, T.M. Rice, Phys. Rev. B **2**, 1324 (1970)
14. W. Metzner, P. Schmit, D. Vollhardt, Phys. Rev. B **45**, 2237 (1992); R. Strack, D. Vollhardt, Phys. Rev. B **46**, 13852 (1992)
15. It was also suggested that a continuous transition takes place in the infinite-dimensional Hubbard model [J. Schlipf, M. Jarrell, P.G.J. van Dongen, N. Blümer, S. Kehrein, T. Prushke, D. Vollhardt, Phys. Rev. Lett. **82**, 4890 (1999)], but an accurate treatment of reference [17] gives the phase coexistence in the low temperature regime and shows that this transition is first order
16. G. Moeller, Q. Si, G. Kotliar, M.J. Rozenberg, D.S. Fisher, Phys. Rev. Lett. **74**, 2082 (1995)
17. M.J. Rozenberg, R. Chitra, G. Kotliar, Phys. Rev. Lett. **83**, 3498 (1999)
18. R. Bulla, T. Pruschke, A.C. Hewson, J. Phys.: Condens. Matter **10**, 8365 (1998); R. Zitzler, N. Tong, T. Pruschke, R. Bulla, `ArXiv:cond-mat/0308202`, unpublished (2003)
19. C. Gros, W. Wenzel, R. Valentí, G. Hülsenbeck, J. Stolze, Europhys. Lett. **27**, 299 (1994)
20. R. Noack, R. Gebhard, Phys. Rev. Lett. **82**, 1915 (1999)
21. J.E. Hirsch, Phys. Rev. B **35**, 1851 (1987)
22. R.T. Scalettar, D.J. Scalapino, R.L. Sugar, D. Toussaint, Phys. Rev. B **39**, 4711 (1989)
23. M. Cyrot, H. Kaga, Phys. Rev. Lett. **77**, 5134 (1996)
24. R. Staudt, M. Dzierzawa, A. Muramatsu, Eur. Phys. J. B **17**, 411 (2000)
25. J.E. Hirsch, S. Tang, Phys. Rev. Lett. **62**, 591 (1989)
26. S. Moukouri, M. Jarrell, Phys. Rev. Lett. **87**, 167010 (2001)
27. R. Preuss, W. Hanke, C. Gröber, H.G. Evertz, Phys. Rev. Lett. **79**, 1122 (1997)
28. E. Arrigoni, G.C. Strinati, Phys. Rev. B **44**, 7455 (1991); R. Frésard, P. Wölfle, J. Phys.: Condens. Matter **4**, 3625 (1992)
29. A. Georges, G. Kotliar, Phys. Rev. B **45**, 6479 (1992); M. Jarrell, Phys. Rev. Lett. **69**, 168 (1992)
30. S.R. White, Phys. Rev. B **46**, 5678 (1992); M. Vekić, S.R. White, Phys. Rev. B **47**, 1160 (1993)
31. As a consequence of the local self-energy, the Green's functions found along the AF BZ are degenerate in the DMFT, while in reality they are only nearly degenerate, as obtained in the 2D-QMC method
32. A.M. Oleś, G. Stollhoff, Phys. Rev. B **29**, 314 (1984)
33. This hysteresis appears in a range of U values in which two locally stable solutions of the DMFT equations exist: a global minimum for the antiferromagnetic state, and a local minimum for the paramagnetic state
34. Equation (8) is based on experimental data, and was introduced by G.S. Rushbrooke, P.J. Wood, Mol. Phys. **1**, 257 (1958); more discussion is given in: "Ferromagnetism" in *Encyclopedia of Physics*, edited by H.P.J. Wijn (Springer, Berlin, 1966), Vol. XVIII/2, pp. 1–273
35. A.W. Sandvik, Phys. Rev. Lett. **80**, 5196 (1998)